

Ratcheting of high temperature materials at thermal cyclic loading

Getsov L., Rybnikov A., Semenov A.

¹NPO TsKTI St. Petersburg, Politechnicheskaja 24, Russia and St.-Petersburg State Polytechnical University, Russia, St.-Petersburg 195213 Zanevskii 43 apt 89

guetsov@online.ru

Keywords: hysteresis loop, thermal-cyclic loading, crystallographic orientation, damage, microcrack, ratcheting

Introduction

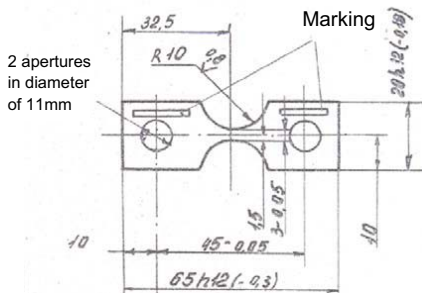
Unilateral accumulation of irreversible strains results in metal to damages under thermal-cyclic loading, in some cases they are commensurable with damages caused by cyclic irreversible strains determined by the width of the hysteresis loop. The safety factors determined by these damages are usually estimated by calculations using the adaptability theory [1]. A lot of publications of the last years cover development of the inelastic models enabling to describe the ratcheting phenomenon under the cyclic loading [2-14].

The present work includes experimental study of the ratcheting in cast polycrystalline and single crystal nickel alloys under thermal-cyclic loading and development of method for forecasting of characteristics of the ratcheting processes in single alloys (depending on the crystallographic orientation). The experiments have been carried with the help of the procedure using specimens with different crystallographic orientation in conditions of cycles with different maximal temperature and cycle duration.

Materials and test method

A comprehensive procedure in NPO CKTI is developed for definition of thermal fatigue resistance of various materials and coatings on the basis of a special appliance which allows to clamp flat sand-glass shaped test-pieces fixedly and to provide their cyclic heating by current conducting (Fig. 1). Heating is executed according to specified program (Fig. 2) maintained automatically during testing. The appliance is fixed in a vacuum-chamber. With vacuum-depth increasing ultimate cycle temperature, defined by the rate of oxide film formation on the sample surface, also increases. Sample material behavior at various surface points is observed with a microscope with magnification x250. During testing the following parameters are determined: characteristic properties of deformation relief defining mechanism of accumulation of thermal-fatigue damages; number of cycles to first microcracks formation in various elements of metal and coating structure; growth rate of incipient cracks; number of cycles to sample failure and accumulated deformations in the ruptured zone.

a)



b)

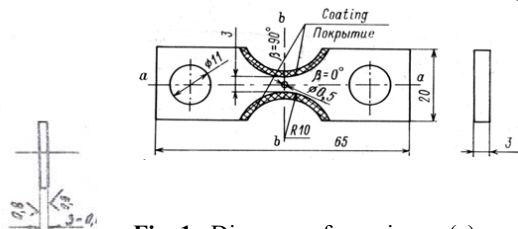


Fig. 1. Diagram of specimen (a) and sketch of the specimen with coating and central hole (b).

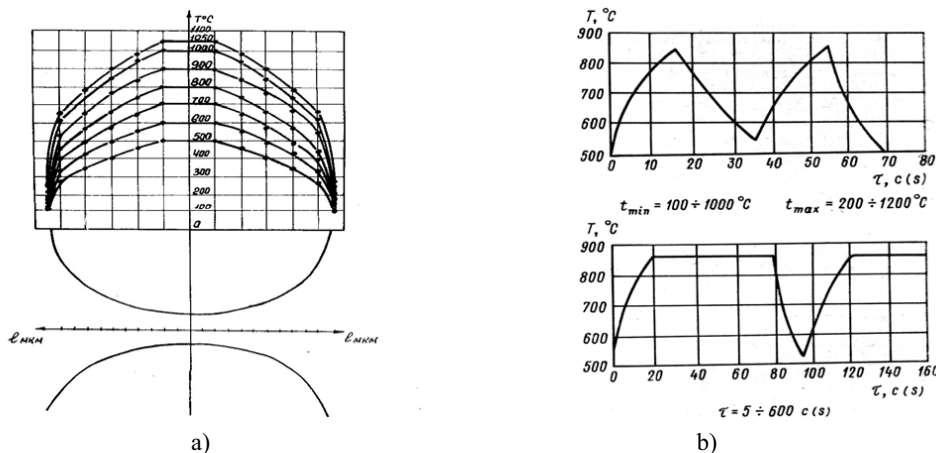


Fig. 2. Experimentally certain distribution of temperature along length of a sample (a) and an example of change of the maximal temperature in a working part of a sample during a cycle (b).

The range of conditionally elastic stresses $\Delta\sigma$ and range of total deformation $\Delta\varepsilon$ in the specimen's working part in the cycle was calculated by the formula

$$\Delta\sigma = (E_{st1}\alpha_1T_{max} - E_{st2}\alpha_2T_{min})\varphi; \Delta\varepsilon = (\alpha_1T_{max} - \alpha_2T_{min})\varphi; \varphi = 1 - \Delta k / \Delta l, \tag{1}$$

here E_{st} - static elastic modulus; Δl - free travel of test points during heating from T_{min} to T_{max} , Δk - measured value of displacement of control micro-hardness marks, applied on the sample surface along its working part edges, during the cycle;

In this calculation the values Δk and φ , were used after being averaged on the basis of the hypotheses of their linear summability.

Tests were spent with polycrystalline and single crystal alloys. Samples from the alloys ZMI-3U and CNK-7 were cut out from polycrystalline casting of turbine blades. Some 9 mm-wide plates made of single crystal alloy with different orientation had been prepared for the tests (see Table 1).

Table 1. Sample orientations

Number of the sample series	Orientation	A deviation from exact orientation, degree	Azimuthal orientation of crystallographic planes, degree
1	111	5,64	8,26
2	011	4,51	11,27
3	011	8,33	14,43
4	011	9,67	7,86
5	001	5,47	41,97

Two technologies were used for manufacturing specimens out of plates: milling (plate N3) and electrospark with preliminary grinding of plates from two sides (plates 1, 2, 4, 5) down to the width 3mm. During grinding some deformations of the plates took place that made it necessary to use special fastening and to turn them over after grinding on the depth 0,1mm. The 0,5 mm holes have

been made with electrospark method. Finally one flat side of each sample had been polished to have a metallographic specimen, which structural changes were observed in the course of the experiment.

Experimental results and their analysis

The experimental results are given in Table 2,3. Here ε_1 и ε_2 - irreversible deformations in the ruptured zone in perpendicular and parallel directions in relation to the metallographic planes.

The obtained data for cast heat resisting polycrystalline and single crystal alloys allows to note the following.

- At thermocyclic loading there is an accumulation of the irreversible deformations which size is comparable to deformation ability of a corresponding alloy. The size of deformations in two directions essentially differs, that is connected with a directivity of structures in cast alloys. Dependence of size of deformation on temperature conditions loading is not observed.
- For samples with the concentrator of pressure deformation of samples from a single crystal alloy of ε_1 less sizes ε_2 that is connected with smaller rigidity of a material in a direction, perpendicular axes of an aperture.
- For samples from a single crystal alloy of series 5 and partially 4 deformation of ε_1 more sizes ε_2 .
- In tests of samples from a single crystal alloy with endurances at T_{\max} the maximum deformation appears more than for tests without endurances. However, when T_{\max} it is that, that creep at it is poorly expressed (850 °C), influence of time of endurance on deformation is shown poorly, The-number of cycles before formation of the first microscopic cracks is much less, than number of cycles before destruction of samples.

Table 2. Results of tests for thermal fatigue of an alloy ZMI-3U

Specimen number	The minimal temperature of a cycle , °C	The maximum temperature of a cycle , °C	Number of cycles to cracks nucleation	Number of cycles before failure	$\Delta\varepsilon$, %	ε_1 , %	ε_2 , %
63-92	150	850	4	291	0,98	14,3	8,7
63-95			17	141	0,99	8,7	16,3
63-BX			16	153	0,92	19,7	4
63HP			16	183	0,91	3,7	22,3
74-6			3	195	0,86	11,3	20,3
74-4			3	405	0,76	6,7	32,7
74-1			2	58	0,84	2,0	8,7
19-5			2	33	-	11	15,7
63-93			250	850	20	690	0,71
63-91	350	850	45	755	0,62	5,3	10,3
74-5	500	850	32	5221	0,43	6,3	22
74-2			2	33	-	-16,7	33
19-6			25	2262	0,45	13,3	27,3
39-17			8	560	0,63	4,3	8,7
63-94			4	415	0,59	6,7	5,7
39-16			400	750	50	5568	-

On the basis of the data, shown in the table, we made the following observations:

For specimen with stress concentrators the deformation ε_1 is less than ε_2 due to the lower stiffness of the material in the direction, perpendicular to the hole's axis. Dependence of the deformation value on the temperature conditions of loading has not been found out,

Table 3. Some results of tests for thermal fatigue of single crystal alloy

Specimen number and orientation		The minimal temperature of a cycle, °C	The maximum temperature of a cycle, °C	Time of stay, min	Number of cycles before failure	ϵ_1 , %	ϵ_2 , %
1-1 with conc.	[111]	150	900	0	50	4,0	24,3
1-2				0	823	6,7	10,7
1-5				2	140	16,3	21
1-7		350	900	5	16	18,3	28
1-6 with conc.				0	320	2,0	16
1-4 with conc.				5	118	4,0	11,7
1-3				2	194	17,7	23,7
2-2	[011]	500	1000	0	472	12	21,3
2-5				5	317	23	29,7
2-1				0	100	15,3	10
2-4 with conc.		350	850	0	2952	6,0	9,3
2-6 with conc.		500	1000	0	187	10,6	10,3
2-3 with conc.				2	62	5,3	13,7
5-1				0	560	9,0	5,3
5-2	[001]	250	1000	0	95	12	6,3
5-3		500	1000	0	1460	12	4,7

The maximum deformation in case of tests with keeping the specimens under maximum cycle temperature is more, than in tests without such keeping. However, when this maximum temperature is not very high (850 °C) and the creep is hardly observable, the effect from keeping the specimens under the such maximal temperature is insignificant,

For the specimens of the group 5 and, partly, of the group 4 the deformation ϵ_1 is higher than ϵ_2 .

Specimen deformation and damage accumulation

With aim to evaluate a durability of specimens the maximum values and amplitudes of stress and strain fields have been numerically calculated. The initial-boundary-value problems have been solved using the finite element method. The stress-strain states of samples were calculated with the help of the software package PANTOCRATOR [16] (see <http://www.pantocrator.narod.ru>), developed in St.-Petersburg State Polytechnical University.

As a mathematical model of the material we used a thermo-visco-elastic micromechanical model in which the presence of slip planes is taken into account. This model represents a generalization of the Taylor model [17]. The constitutive equations are:

$$\begin{aligned}
 \dot{\varepsilon}^p &= \sum_{\alpha=1}^N \dot{\gamma}^\alpha \mathbf{P}^\alpha \\
 \mathbf{P}^\alpha &= \frac{1}{2} (\mathbf{n}^\alpha \mathbf{l}^\alpha + \mathbf{l}^\alpha \mathbf{n}^\alpha) \\
 \dot{\gamma}^\alpha &= A^\alpha |\tau^\alpha|^n \text{sign}(\tau^\alpha) \\
 \tau^\alpha &= \boldsymbol{\sigma} \cdot \mathbf{P}^\alpha \\
 \boldsymbol{\sigma} &= \mathbf{C} \cdot (\boldsymbol{\varepsilon} - \boldsymbol{\varepsilon}^p - \boldsymbol{\varepsilon}^T)
 \end{aligned} \tag{1}$$

where N is the number of slip systems, \mathbf{n}^α are the normals to the slip plane, \mathbf{l}^α are the slip directions, ${}^4\mathbf{C}$ is elastic moduli tensor, τ^α are tangential stresses, reduced to the slip system α .

The following parameters of inelastic deformation are found experimentally:

- Exponent - n ,
- Coefficients of the flow law (analogous to the Norton law) - A^α .

We use the equal values $A^\alpha = A$ for all the slip systems because of absence of necessary detailed experimental data for different slip systems needed for evaluation of A^α . For the further analysis we have chosen the minimum value of A at which a noticeable hysteresis curve can be observed. In all the results shown below we used in the finite-element analysis the following values: $n = 5.95$, $A = 3.78 \cdot 10^{-22}$.

In the crystallographic coordinates the matrix $[\mathbf{S}]$, corresponding to the elastic compliance tensor ${}^4\mathbf{S} = {}^4\mathbf{C}^{-1}$, for the concerned single crystal material looks like:

$$[\mathbf{S}] = \begin{pmatrix} s_{11} & s_{12} & s_{12} & 0 & 0 & 0 \\ s_{12} & s_{11} & s_{12} & 0 & 0 & 0 \\ s_{12} & s_{12} & s_{11} & 0 & 0 & 0 \\ 0 & 0 & 0 & s_{44} & 0 & 0 \\ 0 & 0 & 0 & 0 & s_{44} & 0 \\ 0 & 0 & 0 & 0 & 0 & s_{44} \end{pmatrix} \tag{2}$$

Here the following designations are used: $S_{11} = S_{1111}$, $S_{12} = S_{1122}$, $S_{44} = 2S_{2323}$.

The temperature dependence of the components of the elastic compliance tensor is determined by the relationships [18]:

$$\begin{aligned}
 S_{11} &= 0.7167 \cdot 10^{-5} - 0.2486 \cdot 10^{-9} T + 2.2848 \cdot 10^{-12} T^2, \\
 S_{12} &= -0.2742 \cdot 10^{-5} + 0.1766 \cdot 10^{-9} T + 0.9999 \cdot 10^{-12} T^2, \\
 S_{44} &= 0.7709 \cdot 10^{-5} + 0.5500 \cdot 10^{-9} T + 1.5106 \cdot 10^{-12} T^2,
 \end{aligned} \tag{3}$$

here T is the temperature in $^\circ\text{K}$. The values of the elasticity moduli can be calculated with the help of the following formulae: elasticity modulus $E_{001} = 1/S_{11}$, shear modulus $G_{001} = 1/S_{44}$, Poisson's ratio $\nu = -S_{12}/S_{11}$. The material thermo-elastic properties, used in further finite-element calculations, are presented in Table 4.

Table 4. The thermo-elastic properties at different temperatures.

T , °C	E_{001} , 10^5 MPa	ν	G_{001} , 10^5 MPa	α_{001} , 10^{-6} °C ⁻¹
20	1.372	0.395	1.250	12.4
500	1.199	0.417	1.107	13.8
800	1.049	0.428	0.996	17.1
900	0.998	0.432	0.959	18.1
1000	0.948	0.435	0.921	22.2

The precomputations necessary for the qualitative analysis, were performed (unless otherwise specified) disregarding the temperature dependence of the material mechanical properties. The sample deformation mode under thermal cycle loading is shown in the Fig. 3. The process of barrel-shaping in the middle part is observed.

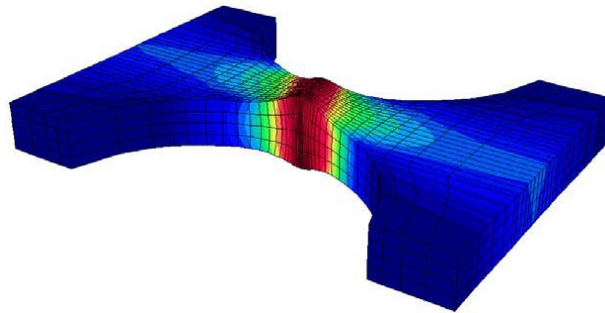


Fig. 3. The deformation state of the sample 3-0 at the 3rd cycle. Displacements 25 times magnified.

The performed calculations have shown, that the dominant strain is ϵ_z , but the values ϵ_x and ϵ_y are also important. ϵ_z predominates, but ϵ_x and ϵ_y do not differ much.

The stay at T_{max} increases considerably the loop breadth and the unilaterally accumulated deformation (see fig.4).

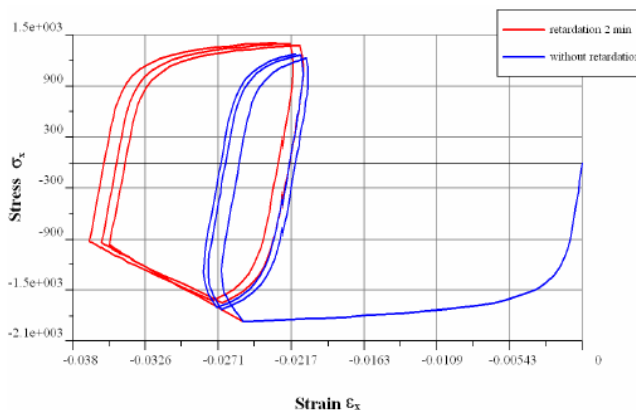
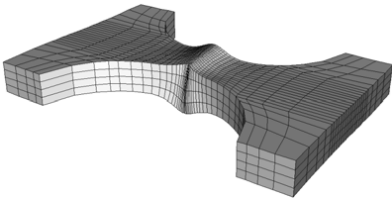
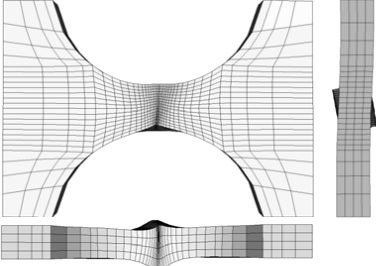
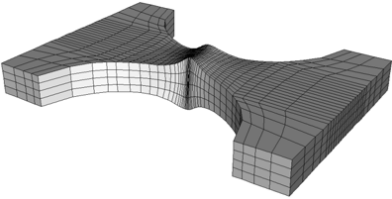
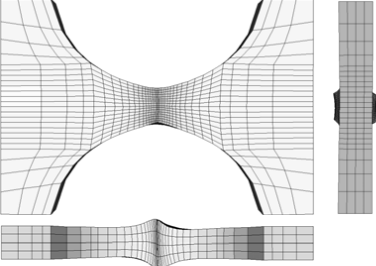
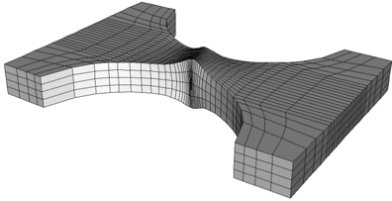
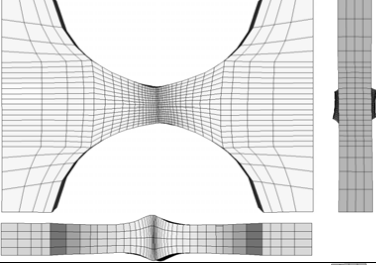
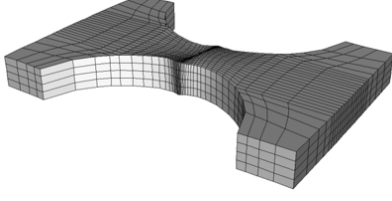
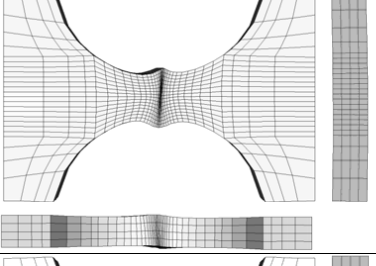
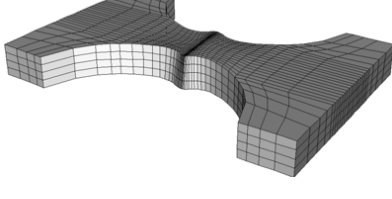
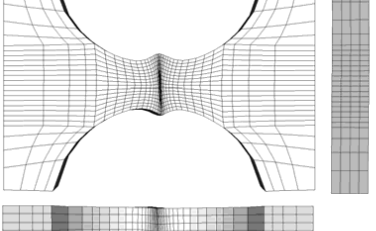


Fig.4. The influence of 2 - minute stay at $T_{max}=900$ °C on the form of the hysteresis curve (sample of series 3, 3 cycles, the central point).

Table 5. The deformation modes for the different specimens (3rd cycle, $T_{min}=150\text{ }^{\circ}\text{C}$). The displacements 30 times magnified.

Simple umber	3D calculations	2D calculations
1-2		
2-1		
3-0		
4-2		
5-1		

For comparison of deformations in specimens with different orientations we used calculations for the loading cycle 150-900 °C (see Table 5). The analysis of obtained data shows, that in the specimens of the groups 2-4 the deformation are mostly accumulated in the direction ϵ_z , whereas in the specimens of the group 5 – mostly in the perpendicular direction, as in the experiment. For the specimen of the group 4 some difference is observed. It can be because of the change of results for greater number of loading cycles.

The researches carried out by Sizova R.N.[20] have shown that, in conditions of compression, the time until fracture is 2,5-3 times longer than in case of tension. When using the deformation criterion of destruction it is equivalent to updating of the ratio $D_3 = \epsilon_{\max}/\epsilon_r$ and $D_4 = \epsilon_{\max}/\epsilon_{cr}$ with the help of correction factor 0,4. Thus, we have:

$$D_3 = 0,4 \epsilon_{\max} / \epsilon_r \quad (4)$$

$$D_4 = 0,4 \epsilon_{\max} / \epsilon_{cr}, \quad (5)$$

where ϵ_r and ϵ_{cr} are correspondingly deformations in case of short-time fracture and fracture in the creep test under T_{\max} under tension.

In table 6 the calculated according to (4) and (5) sizes of damages cast polycrystalline and monocrystal alloys are resulted. Here is $\epsilon_{\max} = \max(\epsilon_1, \epsilon_2)$, where ϵ_1, ϵ_2 – deformations measured in two directions of the sample's cross-section.

Thus, the progressing deformation of samples in tests for thermal fatigue brings the certain contribution to accumulation of the damages, causing reduction of number of cycles before destruction in relation to the durability answering to perfect conditions of rigid loading. It is natural, that for real details the size of the saved up deformations will differ from received in experiment. Therefore there are two exits: (1) to use the received curve resistance of thermal weariness $\Delta\epsilon = f(\log N)$ as giving a certain stock on durability, or (2) to recalculate the values of durability received in experiment with reference to a case of durability towards increase with reference to perfect conditions of rigid loading.

Table 6. Comparison the ratcheting deformation ϵ_{\max} at thermal fatigue and plasticity (short timed plasticity ϵ_{pl} and creep rupture plasticity ϵ_c) at high temperature

Orientation	$T_{\max}, ^\circ\text{C}$	Time of stay, min	$\epsilon_{\max}, \%$	N	ϵ_r % at T_{\max}	ϵ_{cr} % at T_{\max}	D_3	D_4
[001]	900	0	9,0	560	27	12,816,4	0,1	0
	1000	0	12	95	19	8-23	0,25	0
[111]	900	0	10,7 24,3*	823 50	19,5	14-24	0,22	0
		2	21	140			0	0,35-0,6
		5	18,3	16			0	0,3-0,52
	1000	2	23,7	194	21,5	7,2-23,8	0	0,4-1,3

Conclusions

1. The experimental data on accumulation of unilateral irreversible strains in different conditions of thermal-cycle loading have been obtained for the cast polycrystalline alloys and single crystal alloy with different crystallographic orientations.

2. No dependence was found between the maximum cyclic temperature and the accumulated deformation.
3. The specific aspects of strain accumulation have been found out for different crystallographic orientations, cycle period and stress concentration conditions.
4. An elementary thermo-visco-elastic micromechanical model has been used for the simulation of the found effects of the strain accumulation process in single crystals.

References

- [1] Norms of calculation on durability of the equipment and pipelines nuclear. Power installations ПНАЭ Г-7-002-86. M: Energyatomizdat. (1989), 524p.
- [2] Materials Research Society Symp. Proc.: Materials, Technology, and Reliability of Advanced Interconnects, Vol. 863, (2005), P.295-300
- [3] B.Xu, Y.Jiang: Int. J. of Plasticity, (2004), Vol.20, No.12, P.2161-2178.
- [4] X.Feugas, C.Gaudin : Int. J. of Plasticity. Vol. 20, Issues 4-5, (2004), P. 643-662.
- [5] L.Vincent, S.Calloch, D.Marquis: Int. J. of Plasticity, Vol. 20, Issue 10, (2004)
- [6] M.Yaguchi, Y.Takahashi.: Int. J. of Plasticity. Vol. 21, Issue 1, (2004)P.43-65.
- [7] N.Marchal, S.Forest, L.Remy, S.Duvinage: in. Euromech-Mecamat 2006. Local approach to fracture EMMC 9, (2006), P.353-358.
- [8] J.L. Chaboche : Int. J. of Plasticity. (1991), P. 661-678.
- [9] J.L. Chaboche: Eur.J.Mech. A/Solids, (1994), 13, P.501-518.
- [10] L.Bocher, P.Delobelle, P.Robinet, X.Feugas: Int. J. of Plasticity.17, (2001), P.1491-1530.
- [11] Abdel K., Ohao N. Kinematic hardening model suitable for ratcheting with steady – state. (2000), 16, P.225-244.
- [12] S.Bari, T. Hassan.: J. of Plasticity.(2002),18, P.873-894.
- [13] T.H. Lin, K.K.F Wong., N.J.Teng : (Received February 17, 1998; revised October 1, 1999)
- [14] M. M. Shenoy A. P. Gordon., D. L.McDowell, R. W. Neu (Received 5 October 2004; revised 2 February 2005)
- [15] A.I.Rybnikov, L.B Getsov in: *Proceedings of the sixth International congress on thermal stresses*. Vienna, Austria, (May 2005), Vol.1, P.305-309.
- [16] Semenov A.S. in: Proc. V-th Int. Conf. "Scientific and engineering problems of predicting the reliability and service life of structures and methods of their solution", St-Petersburg, (2003). P. 466-480.
- [17] G.I. Taylor . Analysis of plastic strain in a cubic crystal, (1938.) Mc Millan, P. 218-224.
- [18] Single crystals of nickel base superalloys // R.E. Shalin, I.L. Svetlov, E.B.Kachanov and others. M: Machinery, (1997). 333p.
- [19] Getsov L.B. Journal of machinery manufacture under reliability problem, №5, (2001), P. 49-55.
- [20] Thermal strength of machine details. The theory. Experimental researches. Calculation. Edited by I.A. Birger and B.F.. Shorr. M: Mechanical engineering (1975)